

UCLA-00-TEP-15  
 UM-TH-00-07  
 March 2000

# Exact non-factorizable $\mathcal{O}(\alpha_s g^2)$ two-loop contribution to $Z \rightarrow b\bar{b}$

Adrian Ghinculov<sup>a</sup> and York-Peng Yao<sup>b</sup>

<sup>a</sup>*Department of Physics and Astronomy, UCLA,  
 Los Angeles, California 90095-1547, USA*

<sup>b</sup>*Randall Laboratory of Physics, University of Michigan,  
 Ann Arbor, Michigan 48109-1120, USA*

## Abstract

For  $Z \rightarrow b\bar{b}$ , we calculate all the two-loop top dependent Feynman graphs, which have mixed QCD and electroweak contributions that are not factorizable. For evaluating the graphs, without resorting to a mass expansion, we apply a two-loop extension of the one-loop Passarino-Veltman reduction. This is an analytic-numerical method, which first converts all diagrams into a set of ten standard scalar functions, and then integrates them numerically over the remaining Feynman parameters, with rapid convergence and high accuracy. We discuss the treatment of infrared singularities within our methods. We do not resort to unitarity cuts of two-point functions for calculating decay rates; these are useful only to obtain an inclusive rate. For this reason, experimental cuts and the experimental infrared energy resolution can be implemented in our calculation, once the corresponding one-loop gluon Bremsstrahlung process is added to this calculation.

# Exact non-factorizable $\mathcal{O}(\alpha_s g^2)$ two-loop contribution to $Z \rightarrow b\bar{b}$

Adrian Ghinculov<sup>a</sup> and York-Peng Yao<sup>b</sup>

<sup>a</sup>*Department of Physics and Astronomy, UCLA,  
Los Angeles, California 90095-1547, USA*

<sup>b</sup>*Randall Laboratory of Physics, University of Michigan,  
Ann Arbor, Michigan 48109-1120, USA*

## Abstract

For  $Z \rightarrow b\bar{b}$ , we calculate all the two-loop top dependent Feynman graphs, which have mixed QCD and electroweak contributions that are not factorizable. For evaluating the graphs, without resorting to a mass expansion, we apply a two-loop extension of the one-loop Passarino-Veltman reduction. This is an analytic-numerical method, which first converts all diagrams into a set of ten standard scalar functions, and then integrates them numerically over the remaining Feynman parameters, with rapid convergence and high accuracy. We discuss the treatment of infrared singularities within our methods. We do not resort to unitarity cuts of two-point functions for calculating decay rates; these are useful only to obtain an inclusive rate. For this reason, experimental cuts and the experimental infrared energy resolution can be implemented in our calculation, once the corresponding one-loop gluon Bremsstrahlung process is added to this calculation.

High energy experimental data have reached such an accuracy that higher loop effects have to be accounted for. It is increasingly clear that new physics most likely lies beyond the rubric of tree or even one-loop graphs of the standard model.

To assess these higher order effects, in quite a few processes where one can identify a single large scale, a very powerful technique is asymptotic momentum or large mass expansion [1, 3, 4]. This has been applied successfully in several instances, where either the external momenta are small compared to the internal masses, or vice versa. However, in many examples, the external momenta are comparable to the internal scales, and therefore an expansion in their ratios does not apply a priori, or at least is not economical for convergence.

There is a further complication which must be addressed. Massless particles and particles with very small masses are with us. Partly to avoid potential infrared

and mass singularities, many authors calculate inclusive rates, where such issues are by-passed. On the other hand, in a typical experimental setup one needs to make kinematical cuts among other things, and therefore exclusive processes must be considered. It would help if a theoretical calculation can accommodate this.

In a previous article [2] we gave a general framework to calculate any two-loop amplitude with non-trivial interactions. Our approach fully respects the mass structure and the kinematics of the physical process being investigated. The outcome is a standard set of ten functions and their derivatives, arising from tensorial decomposition. Numerical integration over the remaining Feynman parameters is then used for obtaining final results.

In this article we apply this general program to an  $\mathcal{O}(\alpha_s g^2)$  calculation of the process  $Z \rightarrow b\bar{b}$ . So far, this process was calculated by mass expansion methods in refs. [3], with the gluon Bremsstrahlung process integrated over the whole phase space. The calculations already available, being performed at higher order in the mass expansion, show that the expansion methods work well in this particular process. For this reason, it is to be expected that the numerical output of the calculation described in this paper will not result in a sizeable difference from the existing results of ref. [3]. Our emphasis here is more on an illustration, based on an important physical process, of how our two-loop methods work, because the whole machinery deployed covers almost all typical situations, including particles with various masses, two- and three-point functions, and treatment of infrared singularities.

A complete two-loop calculation of the exclusive  $Z \rightarrow b\bar{b}$  decay consists of two technically different parts, namely the pure two-loop part, and the evaluation of the one-loop Bremsstrahlung process. In this paper we treat the mixed QCD-electroweak non-factorizable two-loop contributions to this process. Technically this is the most difficult part of a complete top-dependent  $\mathcal{O}(g^2\alpha_s)$  calculation because it is the part involving massive two-loop diagrams. Of course, for obtaining an infrared finite result one needs to add the gluon emission graphs. The remaining factorizable and Bremsstrahlung diagrams can be calculated by conventional methods. The  $\mathcal{O}(g^2\alpha_s)$  gluon emission process involves four-point one-loop diagrams, for which standard techniques such as the Passarino-Veltman reduction can be used. Here we concentrate only on the pure two-loop part of the calculation, for which special massive two-loop methods are necessary.

The coupling of the  $Z$  boson to a  $b$  quark pair is given by:

$$-i\frac{g}{2\cos\theta_W}\gamma_\mu(v_d - a_d\gamma_5) \quad , \quad (1)$$

which results into a  $Z \rightarrow b\bar{b}$  width given by the following expression:

$$\Gamma_{Z \rightarrow b\bar{b}} = \frac{g^2}{16\pi\cos^2\theta_W} M_Z (|v_d|^2 + |a_d|^2) \quad . \quad (2)$$

The tree level values  $a_d^{(tree)} = -1/2$  and  $v_d^{(tree)} = -1/2 + 2/3\sin^2\theta_W$  receive both

QCD and electroweak radiative corrections.

The two-loop graphs which contribute to the  $Z \rightarrow b\bar{b}$  decay to this order are shown in fig. 1. In the following we calculate these graphs for finite  $Z$ ,  $W$ , and top masses, without using a mass or external momentum expansion. The only approximation we do in this calculation is to neglect the  $b$  quark mass, where this is justified. We use this approximation because its effect is very small, of the order of  $m_b/M_{Z,W,t}$ . This approximation simplifies the intermediary expressions resulting from the tensor reduction of the diagrams. However, we note that including a finite  $b$  mass throughout our calculation would be straightforward.

The first step in calculating these diagrams, after some trivial Dirac algebra, is to decompose the resulting tensor integrals into a set of standard scalar integrals. This is done along the lines of ref. [2]. All tensor structures can be reduced to a set of ten scalar functions  $\mathcal{H}_1 - \mathcal{H}_{10}$ , whose definitions are given in ref. [2].

In carrying out this scalar decomposition procedure, there is a subtlety related to the apparent introduction of some spurious singularities. To illustrate this issue, let us consider a general tensor integral, which is of the following type (see ref. [2]):

$$\int d^n p d^n q \frac{p^{\mu_1} \dots p^{\mu_i} q^{\mu_{i+1}} \dots q^{\mu_j}}{(p^2 + m_1^2)^{\alpha_1} (q^2 + m_2^2)^{\alpha_2} [(r+k)^2 + m_3^2]^{\alpha_3}} . \quad (3)$$

In the expression above, all momenta are rotated to Euclidian. Such a tensor integral can always be decomposed into Lorentz invariant integrals of the type:

$$\int d^n p d^n q \frac{(p \cdot k)^a (q \cdot k)^b}{(p^2 + m_1^2)^{\alpha_1} (q^2 + m_2^2)^{\alpha_2} [(r+k)^2 + m_3^2]^{\alpha_3}} \quad (4)$$

by decomposing the loop integration momenta  $p$  and  $q$  into components parallel and orthogonal to the external momentum  $k$  of the two-loop integral:

$$p_\perp^\mu = p^\mu - \frac{p \cdot k}{k^2} k^\mu , \quad q_\perp^\mu = q^\mu - \frac{q \cdot k}{k^2} k^\mu . \quad (5)$$

However, in doing this, one apparently introduces light-cone singularities of the type  $1/k^2$ . At the same time, it is obvious that the original tensor integral of eq. 3 is free of such singularities, and in fact it can be evaluated analytically at vanishing external momentum for any combination of masses [2]. This obviously means that the scalar integrals which result from the tensor decomposition must have such a  $k^2$  behaviour as to compensate the  $1/k^2$  singularities which result upon introducing the orthogonal loop momenta defined in eqns. 3. Indeed, one can convince oneself that  $1/k^2$  light-cone singularities are non-existent when the tensor integrals are reduced into scalar  $\mathcal{H}_i$  functions. As an example, we give here the tensor decomposition of a two-loop integral with three indices:

$$\int d^n p d^n q \frac{p^\mu q^\nu q^\lambda}{[(p+k)^2 + m_1^2]^2 (q^2 + m_2^2) (r^2 + m_3^2)} =$$

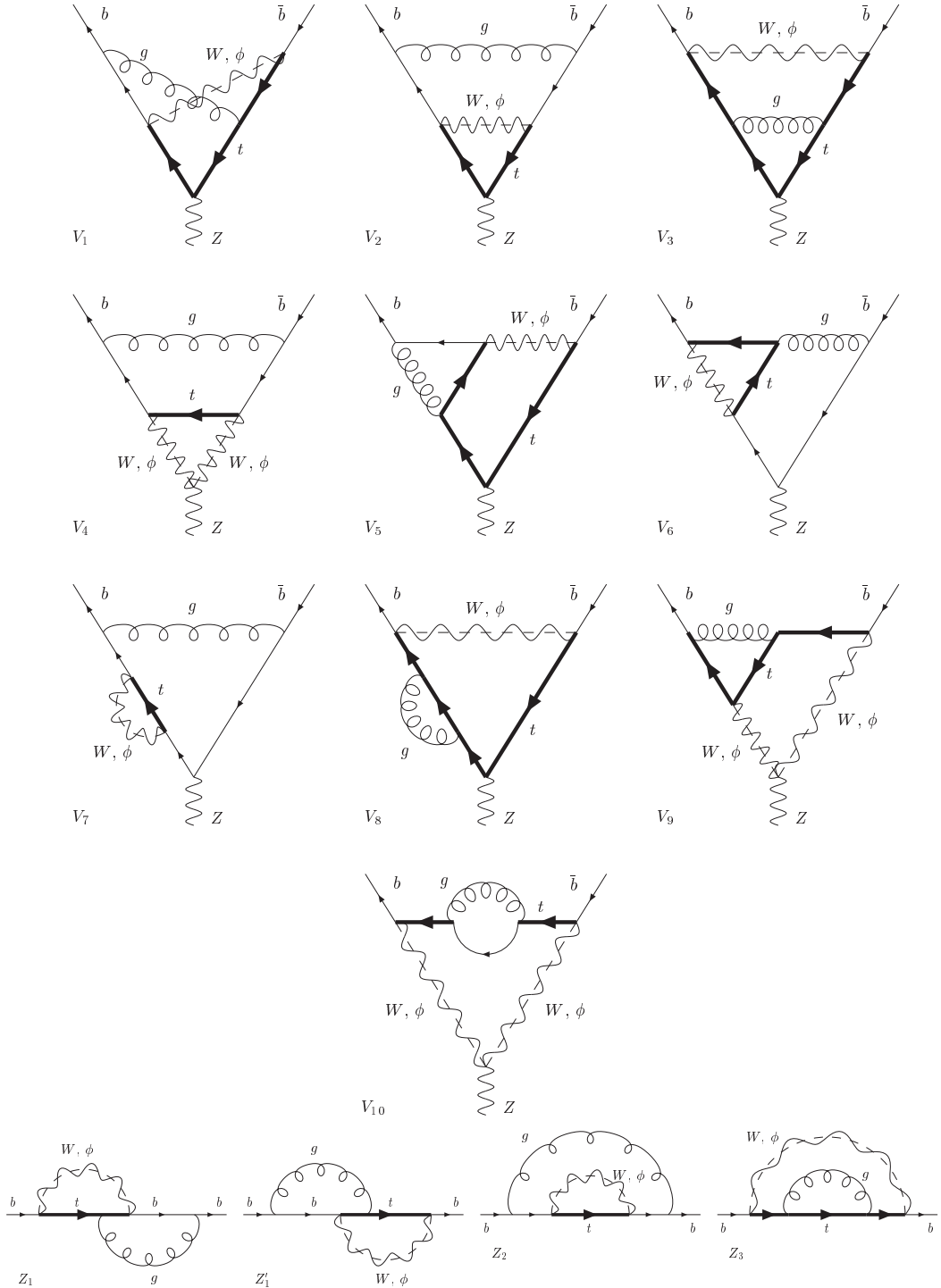


Figure 1: The three- and two-point two-loop Feynman graphs which contribute to the top-dependent correction of  $\mathcal{O}(\alpha_s g^2)$  to  $Z \rightarrow b\bar{b}$ . Diagrams  $V_{1,5,6,7,8,9}$  occur together with the diagrams obtained by reverting the fermion line, which are not shown explicitly.

$$\begin{aligned}
& (\tau^{\mu\nu}k^\lambda + \tau^{\mu\lambda}k^\nu + \tau^{\nu\lambda}k^\mu) \left[ -\left(\frac{1}{k^2}\right)^2 \frac{n+2}{3(n-1)} \mathcal{H}_9 \right] \\
& + (g^{\mu\nu}k^\lambda + g^{\mu\lambda}k^\nu + g^{\nu\lambda}k^\mu) \left[ \left(\frac{1}{k^2}\right)^2 \frac{1}{3} \tilde{\mathcal{P}}_{211}^{12} \right] \\
& + (g^{\mu\nu}k^\lambda + g^{\mu\lambda}k^\nu - 2g^{\nu\lambda}k^\mu) \left\{ \frac{1}{k^2} \frac{1}{3} \left[ \tilde{\mathcal{P}}_{211}^{11} + \tilde{\mathcal{P}}_{211}^{02} - \frac{n}{n-1} (\mathcal{H}_5 + \mathcal{H}_6) \right] \right\}
\end{aligned}$$

where

$$\tau^{\mu\nu} = g^{\mu\nu} - \frac{k^\mu k^\nu}{k^2} \quad (6)$$

with the scalar functions  $\mathcal{H}$  and  $\tilde{\mathcal{P}}$  defined in ref. [2]. By using the explicit expressions of the  $\mathcal{H}$  and  $\tilde{\mathcal{P}}$  functions, one can easily see that this decomposition is indeed free of singularities at  $k^2 \rightarrow 0$ . Singularity-free decomposition formulae are obtained in a similar way for all other tensor integrals involved.

We encoded all the necessary Dirac algebra into an algebraic manipulation program (we used both FORM and Schoonship). The computer program then uses the two-loop reduction algorithm which we described in detail in ref. [2]. Thus it reduces the two-loop Feynman graphs into a set of standard scalar integrals. The final output of the algebraic program is a combination of the special functions  $h_i$ , which are the finite parts of the two-loop scalar integrals  $\mathcal{H}_i$  — see ref. [2].

These final algebraic expressions are directly suitable for further numerical integration. To do this, they are transferred into a FORTRAN integration package [6]. The numerical package can calculate efficiently and with high numerical accuracy the functions  $h_i$ , starting from their integral representations. Then it performs the numerical integration over the remaining Feynman parameters. For achieving both a high integration speed and a high accuracy of the final result, the complex singularities of the integrand are found automatically, and then a smooth complex integration path is automatically calculated in terms of spline functions. Then, along this complex path, an adaptative deterministic algorithm is used, which leads to an accurate numerical evaluation of the Feynman graph.

Collecting all proper vertex contributions shown in figure 1 (diagrams  $V_1$ – $V_{10}$ ), we obtain a correction to the  $Z b \bar{b}$  vertex of the type  $\gamma_\mu(1 - \gamma_5)A^{(vertex)}$  in the massless  $b$  limit.

From the  $b$  self-energy diagrams we derive a  $b$  wave function renormalization contribution. Denoting the  $b$  self-energy by  $i\Sigma(p)$ , we have in general:

$$\Sigma(p) = [A(p^2) + \gamma_5 A_5(p^2)] \gamma \cdot p + B(p^2) + \gamma_5 B_5(p^2) . \quad (7)$$

For the general case of a finite  $b$  mass, the coefficients  $A(p^2)$  and  $A_5(p^2)$ , and the momentum derivatives of  $B(p^2)$  and  $B_5(p^2)$  at  $p^2 = m_b^2$  are needed for extracting the  $b$  wave function renormalization contribution. In ref. [7] we have shown how this can be done within our two-loop formalism. As a side remark, we note here that the on-shell

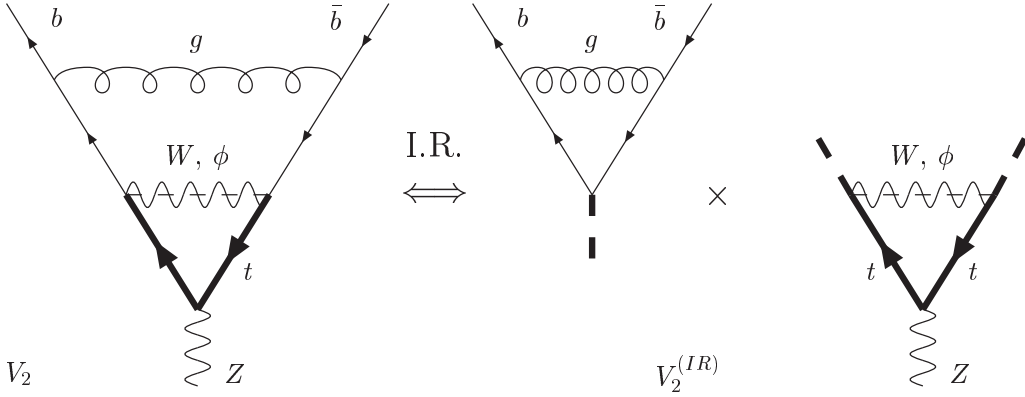


Figure 2: *Extracting the infrared divergent pieces of the two-loop diagrams analytically. The infrared divergency of the two-loop diagram is the same as the infrared divergency of the product of the two one-loop diagrams obtained by “freezing” the common line in the loop momenta integration.*

external momentum differentiation can be best performed by working on the integrand before the momentum integrations [7]. This reduces the size of the expressions which appear at intermediate stages of the calculation, and provides for a systematic treatment of all diagrams. The result for the two-loop wave function renormalization constant is again a set of the ten standard functions we have introduced.

In the massless  $b$  quark limit, the expressions of the self-energy diagrams simplify considerably. The self-energy simplifies to  $\Sigma(p) = A(p^2)(1 + \gamma_5)\gamma \cdot p$ . Accordingly, the  $b$  wave function renormalization constant contribution to the  $Zb\bar{b}$  vertex correction reads  $\gamma_\mu(1 - \gamma_5)(a_d^{tree} + v_d^{tree})A(p^2 = 0)$ .

Therefore, the non-factorizable two-loop contributions of figure 1 contribute a correction

$$\gamma_\mu(1 - \gamma_5) [A^{(vertex)} + (a_d^{tree} + v_d^{tree})A(p^2 = 0)] \quad (8)$$

to the  $Zb\bar{b}$  vertex.

At this point we would like to discuss the treatment of infrared divergencies. Among the three-point diagrams,  $V_2$ ,  $V_4$ ,  $V_6$ , and  $V_7$  are infrared divergent. Their infrared divergencies can be isolated analytically in the way shown in figure 2 for the case of  $V_2$ . The analytical isolation of infrared singularities is based on the observation that the original two-loop diagram has one line common for the two loop momenta which are to be integrated out — the  $W/\phi$  line in the case of diagram  $V_2$ . By “freezing” the loop integration momentum of this internal line to the value of the loop momentum whose one-loop sub-diagram is infrared finite — the  $ttW$  triangle sub-diagram in the case of diagram  $V_2$  — one obtains a product of two one-loop diagrams which has precisely the same infrared singularities as the two-loop diagram. All other infrared divergent diagrams can be treated in the same way.

The analytical infrared isolation and factorization into one-loop diagrams clearly works nicely for all two-loop diagrams involved in the  $Z \rightarrow b\bar{b}$  calculation, shown in figure 1. However, it is an open question if this can be done in *all possible* two-loop cases, and especially in the case of calculations of higher order in  $\alpha_s$ , such as two-loop pure QCD calculations. This point clearly deserves further investigation. We note that our massive two-loop reduction scheme is mainly designed for *massive* calculations; for pure QCD calculations other methods which take advantage of the massless structure of the theory may prove more efficient — see for instance ref. [5] for a few recent examples.

Once the infrared singularities are isolated and written in the form of one-loop diagrams, one chooses a regularization method to treat them and cancel them upon the real gluon emission process. Dimensional regularization is often used in higher-order QCD calculations. Given that the process considered here is only of  $\mathcal{O}(\alpha_s)$  in the strong coupling constant, a second possibility is to use a gluon mass regulator. This does not upset the Slavnov-Taylor identities for our case because to the order considered here the infrared structure is the same as in the Abelian case.

Independently of the choice for the infrared regulator, separating the infrared singular piece analytically is useful for increasing the efficiency of the numerical integration of the two-loop diagram. For instance, in the case of diagram  $V_2$  discussed in figure 2, the infrared singularity appears as an end-point singularity in a two-fold Feynman parameter integration. By subtracting first the product of two one-loop diagrams shown in figure 2, this end-point singularity is being removed and the numerical integration over the resulting smooth function ( $V_2 - V_2^{(IR)}$ ) becomes much more efficient than  $V_2$  alone.

In the following discussion it is understood that the infrared singularities are regularized by introducing a gluon mass regulator  $m_g$ . Again, we would like to stress that dimensional regularization can be used equally well.

When calculating the two-loop diagrams of figure 1, we deal with infrared divergences in the form of  $\text{Lim}_{m_g \rightarrow 0} \ln(m_g)$ , where  $m_g$  is the gluon mass regulator. These infrared divergent terms cancel those from real gluon emission when we calculate a decay rate, and we have checked this explicitly. The net effect of this cancellation is to replace the gluon mass regulator  $m_g$  by the maximum undetected gluon energy, or the energy resolution of an experiment  $\omega_{max}$  — the logarithmic infrared behaviour is universal and we do not need to calculate explicitly the Bremsstrahlung process to extract it. Of course, after the infrared cancellation one is left with a finite piece and an explicit calculation of the real gluon emission process is needed. This involves the evaluation of four-point one-loop diagrams and integration over three-particle phase space with the appropriate experimental cuts. The Bremsstrahlung process is beyond the scope of this article — we only note that the calculation can be performed with conventional methods such as the Passarino-Veltman reduction.

In figure 3 we give numerical results for the pure two-loop contribution to the  $Z \rightarrow b\bar{b}$  amplitude, stemming from the diagrams shown in figure 1. Instead of plotting

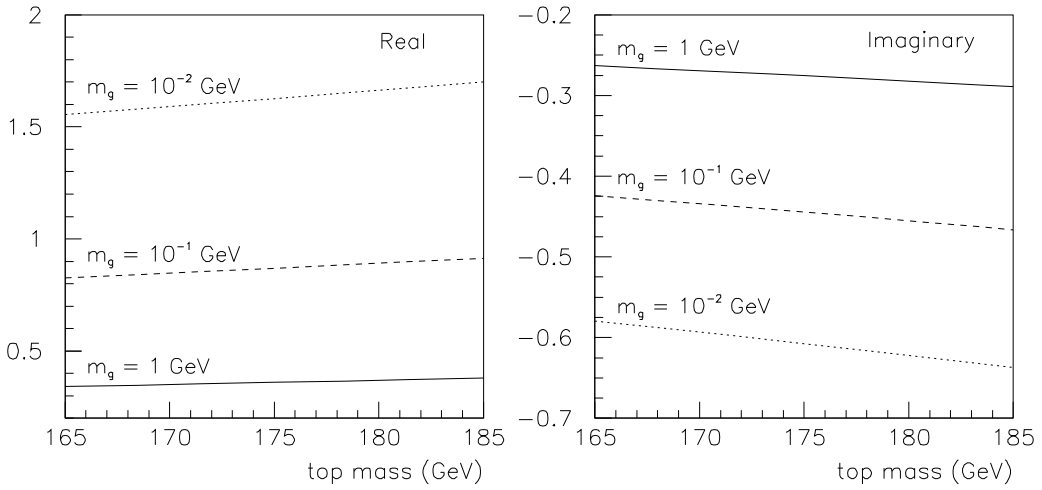


Figure 3: *Numerical results for the pure two-loop contribution due to the proper Feynman graphs given in figure 1 (see the text). The ultraviolet poles are removed by minimal subtraction. The infrared divergencies are separated as one-loop integrals and can be handled either by dimensional regularization or by using a gluon mass regulator  $m_g$ . Here we give numerical results for a range of  $m_g$ . An overall colour and coupling constant factor of  $i\alpha_s(g^3/12 \cos \theta_W)$  is understood.*

each diagram separately, we give their total contribution, which translate into the term  $[A^{(vertex)} + (a_d^{tree} + v_d^{tree})A(p^2 = 0)]$  of eq. 8. All diagrams are subtracted in the ultraviolet by minimal subtraction. We have checked explicitly that the ultraviolet infinities are absorbed into the mass, coupling constant, and wave function renormalization. This serves as a good check on the two-loop tensor decomposition algebra. The infrared divergencies are regulated by using a gluon mass regulator. Should dimensional regularization of infrared singularities be preferred, this is straightforward to implement by correspondingly treating the one-loop infrared pieces of the type shown in figure 2. We used  $M_Z = 91.187$  GeV,  $M_W = 80.41$  GeV, and the effective electroweak mixing angle  $\sin^2 \theta = .2312$ .

In conclusion, we calculated all two-loop proper diagrams relevant for the  $\mathcal{O}(\alpha_s g^2)$  top-dependent correction to the  $Z \rightarrow b\bar{b}$  decay width, by using two-loop methods which we developed previously. We have developed an on-shell momentum expansion which allows for a simple extraction of wave function renormalization constants. We discussed the isolation of infrared singularities in the form of products of one-loop integrals. This allows the treatment of infrared cancellations with the Bremsstrahlung process either by dimensional regularization or by using a gluon mass regulator which is legitimate in this particular order. Our calculation is exact, in the sense that we do not rely upon mass or momentum expansions of Feynman diagrams — we rather calculate them at finite mass and momentum values from the outset. Being based

on a general algorithm, the calculation presented in this contribution opens the way for the calculation of a number of other two-loop corrections which have become necessary because of improved experimental electroweak data.

### Acknowledgements

The work of A.G. was supported by the US Department of Energy. The work of Y.-P. Y. was supported partly by the US Department of Energy.

## References

- [1] Y. Kazama and Y.-P. Yao, *Phys. Rev.* **D21** (1980) 1116; V.A. Smirnov, *Renormalization and Asymptotic Expansions*, Birkhauser, Basel (1991).
- [2] A. Ghinculov and Y.-P. Yao, *Nucl. Phys.* **B516** (1998) 385.
- [3] J. Fleischer, O.V. Tarasov, F. Jegerlehner, P. Raczka, *Phys. Lett.* **B293** (1992) 437; R. Harlander, T. Seidensticker, M. Steinhauser, *Phys. Lett.* **B426** (1998) 125; J. Fleischer, F. Jegerlehner, M. Tentyukov, O. Veretin, *hep-ph/9904256*.
- [4] G. Degrassi, F. Feruglio, A. Vicini, S. Fanchiotti, P. Gambino , *Phys. Lett.* **B350** (1995) 75; G. Degrassi, S. Fanchiotti, P. Gambino, *Int. J. Mod. Phys.* **A10** (1995) 1337.
- [5] V.A. Smirnov, O.L. Veretin *Nucl. Phys.* **B566** (2000) 469; J.B. Tausk, *Phys. Lett.* **B469** (1999) 225; C. Anastasiou, T. Gehrmann, C. Oleari, E. Remiddi, J.B. Tausk, *hep-ph/0003261*; Z. Bern, L. Dixon, D.A. Kosower, *JHEP* **0001** (2000) 027; J.A.M. Vermaseren, S.A. Larin, T. van Ritbergen, *Phys. Lett.* **B405** (1997) 327; *Phys. Lett.* **B404** (1997) 153; *Phys. Lett.* **B400** (1997) 379.
- [6] A. Ghinculov and J.J. van der Bij, *Nucl. Phys.* **B436** (1995) 30; A. Ghinculov, *Phys. Lett.* **B337** (1994) 137; (E) **B346** (1995) 426; *Nucl. Phys.* **B455** (1995) 21; A. Ghinculov and Y.-P. Yao, *hep-ph/0002211* .
- [7] A. Ghinculov and Y.-P. Yao, *hep-ph/9910422*.